HHS Public Access

Author manuscript

Prostate. Author manuscript; available in PMC 2020 August 01.

Published in final edited form as:

Prostate. 2019 August ; 79(11): 1256–1266. doi:10.1002/pros.23829.

Distinct expression patterns of SULT2B1b in human prostate epithelium

Jiang Yang[1], **Meaghan M. Broman**[1], **Paula O. Cooper**[1], **Nadia A. Lanman**[1,2], **Douglas W. Strand**[3], **Colm Morrissey**[4], **Timothy L. Ratliff**[1,2]

[1]Department of Comparative Pathobiology, College of Veterinary Medicine, Purdue University, West Lafayette, Indiana

[2]Purdue Center for Cancer Research, Purdue University, West Lafayette, Indiana

[3]Department of Urology, UT Southwestern Medical Center, Dallas, Texas

[4]Department of Urology, University of Washington, Seattle, Washington

Abstract

Background: SULT2B1b (sulfotransferase family cytosolic 2B member 1b) catalyzes the sulfate conjugation of substrates such as cholesterol and oxysterols. Our laboratory has previously shown that SULT2B1b inhibition modulates androgen receptor signaling and induces apoptosis in prostate cancer cells. However, the functions of SULT2B1b in the prostate remain poorly understood.

Methods: We characterized the expression pattern of SULT2B1b in human benign prostate hyperplasia (BPH) as well as prostate cancer to determine the relationship between SULT2B1b and prostate diseases, using immunohistochemistry, immunofluorescence staining, immunoblot, and real-time polymerase chain reaction.

Results: SULT2B1b was strongly detected in the prostate epithelium but was absent in the stroma. Significantly lower SULT2B1b was found in primary cancer cells compared with adjacent normal epithelial cells. SULT2B1b further decreased in metastatic cancer cells. Most interestingly, we found, for the first time, that SULT2B1b was much more concentrated in the luminal layer than in the basal layer in both normal prostate and BPH samples. The stronger presence of SULT2B1b in luminal epithelial cells was confirmed by costaining with luminal and basal markers and in sorted paired luminal and basal cells. SULT2B1b expression was induced with prostate organoid differentiation.

Conclusions: SULT2B1b inversely correlates with prostate cancer status, with the highest level in the normal epithelium and lowest in the advanced metastatic prostate cancer. Furthermore,

Correspondence Timothy L. Ratliff, Distinguished Professor of Comparative Pathobiology, Robert Wallace Miller Director, Purdue University Center for Cancer Research, Hansen Life Sciences Research Building, 201 S. University Street, West Lafayette, IN 47907-2064. tlratliff@purdue.edu.

SUPPORTING INFORMATION

Additional supporting information may be found online in the Supporting Information section.

CONFLICT OF INTERESTS

The authors declare that they have no conflict of interests.

SULT2B1b is mostly located within the luminal layer of the prostate epithelium, suggesting that it may be implicated in luminal differentiation.

Keywords

basal; benign prostate hyperplasia; luminal; prostate cancer

1 | INTRODUCTION

SULT2B1b is one of the two isoforms of SULT2B1 (sulfotransferase family 2B member 1). It is slightly longer at the N-terminus than the other isoform SULT2B1a due to alternative splicing.[1] Although both isoforms can be detected at the transcript level, SULT2B1a cannot be detected in human tissues at the protein level.[2] SULT2B1b preferentially catalyzes the addition of a sulfate group to cholesterol, generating cholesterol sulfate.[3] The other known substrates of SULT2B1b include oxysterols, the hydroxylated derivatives of cholesterol.[4] Oxysterols act as ligands for the liver X receptor (LXR) and SULT2B1b-mediated sulfonation inactivates oxysterols as LXR ligands and therefore inhibits LXR signaling.[5] Cholesterol sulfate (CS) has been shown to be critical for the differentiation and barrier function of skin epidermis.[6] The genetic mutations that lead to SULT2B1 deficiency have been linked to ichthyosis, a skin disorder.[7] The presence of CS has been shown to interfere with the functions of cholesterol. For example, CS displaces cholesterol from T cell membrane, disrupting the interaction between cholesterol and T cell receptors and preventing the receptors from normal functioning.[8] CS may also perform functions that are independent of cholesterol.[9]

The prostate epithelium is composed of a secretory luminal layer and a basal layer that sits on the basement membrane. Luminal and basal epithelial cell populations each express a distinct set of markers, recently delineated by single-cell RNA sequencing.[10] For identification in situ, luminal epithelial cells have historically been identified by cytokeratin 8/18 and PSA (prostate-specific antigen) expression, whereas basal cells express cytokeratin 5/14 and p63.[11] Benign prostate hyperplasia (BPH) is predominantly due to the expansion of the luminal epithelial cells (glandular hyperplasia) with 8% to 10% of BPH cases due to the hyperplasia of the basal layer (basal hyperplasia).[12-14] Luminal and basal epithelial cells have both been identified as the cell of origin for prostate cancer,[15] with basal cells being linked with more aggressive prostate cancer.[16] Prostate cancer with luminal or basal subtypes also exhibits different responses to therapies such as androgen deprivation therapy.[17] Understanding the mechanisms by which the luminal or basal phenotype is established or maintained in the prostate can potentially lead to the discovery of new therapeutic targets for both BPH and prostate cancer.

Our laboratory has previously shown that SULT2B1b colocalizes with CS in human prostate cancer tissue samples and that reducing SULT2B1b in human prostate cancer cells (such as LNCaP, VCaP, and C4-2) leads to apoptosis and inhibition of androgen receptor signaling.[18] However, the functions of SULT2B1b in prostate cancer remain poorly understood. Furthermore, there have not been any comprehensive characterization studies of SULT2B1b in the prostate across different pathological conditions. To gain more insight into the

functions of SULT2B1b in the prostate and the underlying mechanisms, we examined the expression pattern of SULT2B1b not only in human prostate cancer, but also in normal prostate and BPH samples. We have found that SULT2B1b is highly expressed in normal prostate and BPH and its expression decreases in prostate cancer and inversely correlates with cancer progression. Most importantly, we have found, for the first time, that SULT2B1b are more concentrated in the luminal layer of the prostate epithelium than the basal layer, suggesting that this protein may be implicated in the differentiation of prostate epithelium.

2 | MATERIALS AND METHODS

2.1 | Human samples

Human prostate tissue microarrays (two arrays with 40 primary tumors and adjacent normal tissues and one array with 42 prostate cancer metastases from bone and other organs, including liver, lung, and lymph nodes, from 21 patients) were constructed at the University of Washington. Detailed information on these arrays is included in Table S1. The metastasis specimens were obtained within 8 hours of death from patients who died of metastatic CRPC (castration-resistant prostate cancer), under the aegis of the Prostate Cancer Donor Program at the University of Washington. Specimens (normal prostate, BPH with glandular and basal hyperplasia) used for SULT2B1b immunohistochemistry and immunofluorescent staining were obtained from patients undergoing transurethral resection or simple prostatectomy for symptomatic BPH at the University of Texas Southwestern Medical Center. BPH specimens used for basal and luminal epithelial cell sorting were obtained from Indiana University Health Methodist Hospital and Indiana University Tissue Procurement Core. All human specimens were acquired under protocols approved by the Institutional Review Boards at each institution.

2.2 | Cell lines

Construction and characterization of LNCaP human prostate cancer cells with tetracycline-inducible SULT2B1b have been previously described by our group.[18] These cells were maintained in Roswell Park Memorial Institute (RPMI) 1640 medium (HyClone, GE Healthcare, Uppsala, Sweden) supplemented with 10% fetal bovine serum (FBS; Corning, Corning, NY). SULT2B1b expression was induced by treating these cells with 1 μg/mL doxycycline for 72 hours. The cells were then trypsinized, pelleted, and fixed in 10% neutral buffered formalin before being embedded in paraffin and sectioned.

2.3 | Immunohistochemistry and immunofluorescence staining

Paraffin slides were deparaffinized and rehydrated on a Leica Autostainer XL (Leica Biosystems, Wetzlar, Germany). Antigen retrieval was performed in 0.05% citraconic anhydride at pH 7.4 using a steamer for 20 minutes at 95°C. Slides were cooled for 20 minutes at room temperature (RT) and rinsed in Tris-buffered saline with Tween (TBST). Immunohistochemistry and immunofluorescence staining protocols were then carried out using a Dako Autostainer Plus (Agilent Technologies, Santa Clara, CA).

For immunohistochemistry, the slides were first incubated with mouse anti-SULT2B1 antibody from Abcam (Cambridge, MA) (#ab88085, 1:8000 dilution) or mouse IgG (Vector

Laboratories, Burlingame, CA) for 30 minutes and then the secondary antibody ImmPRESS horse anti-mouse antibody (Vector) for 30 minutes and finally developed with ImmPACT DAB Substrate Kit (Vector), with TBST rinses between these incubations. Once stained, a Gill's hematoxylin counterstain, dehydration, clearing, and coverslipping were done on the Leica Autostainer XL (Leica). The images were taken using the Leica Aperio system (Leica). The intensity of SULT2B1b staining was graded by a pathologist with no knowledge of sample identity on a scale from 0 to 4 with ascending staining intensity (0, no staining; 4, the strongest staining intensity).

For immunofluorescence staining, slides were first incubated with primary antibodies, including mouse anti-SULT2B1 (Abcam, #ab88085, 1:8000 dilution), rabbit anti-cytokeratin 5 (CK5), and mouse anti-cytokeratin 8 (CK8) antibodies (BioLegend, San Diego, CA). The secondary antibodies used were Alexa Fluor 647 donkey anti-mouse antibody (Invitrogen, Thermo Fisher Scientific, Waltham, MA) for SULT2B1, DyLight 488 horse anti-rabbit antibody (Vector) for CK5, and unconjugated goat anti-mouse antibody (Vector) followed by DyLight 594 horse anti-goat antibody (Vector) for CK8. After staining, the slides were mounted with ProLong Gold Antifade Mountant with 4',6-diamidino-2-phenylindole (DAPI; Invitrogen). The images were taken using the Leica Aperio System (Leica).

2.4 | Analysis of TCGA data

Prostate adenocarcinoma (PRAD) data was downloaded from TCGA (The Cancer Genome Atlas) (http://cancergenome.nih.gov/) in the form of HTSeq raw gene expression counts,[19] which had been aligned to the GRCh38 version of the human genome. The Genomic Data Commons Data Portal API (GDC, https://portal.gdx.cancer.gov/) was used in downloading the data. In comparing tumor and normal samples, due to the large number of samples used for our analysis (497 tumor and 52 normal samples), quantile normalization was used in normalizing counts. Due to the inherent noise in tumor samples, samples were also filtered according to their Spearman correlation between replicate samples. Samples that had a lower Spearman correlation with other samples within the same group less than 0.6 were excluded from the analysis. In quantile normalization, the quantile cut-off used was 0.25 and a false discovery rate of 5% was used.

In the survival analysis, a univariate Kaplan-Meier survival analysis method was used for 497 patients. Two thresholds for quantile expression of SULT2B1 were used in all samples to divide samples into “high” and “low” SULT2B1 expression groups. A cut-off of 0.67 was used as the top quantile threshold to identify samples with high expression of SULT2B1 and 0.33 used as the quantile threshold to identify samples with low expression. A total of 177 samples were in the “high” expression group and 177 samples were in the “low” expression group.

2.5 | Isolation of human prostate basal and luminal epithelial cells

Isolation methods were adapted from Strand et al.[20] Briefly, samples were minced to a paste in the digestion medium (25 U/mL Collagenase type I (Gibco, Thermo Fisher), 0.25 mg/mL Dispase (Gibco) in RPMI 1640 medium with 10% FBS). Using 5 mL per 200 mg tissue, samples were incubated overnight in 50 mL tubes at 37°C with shaking and were spun down

at 200 g for 5 minutes. Samples were next incubated in TrypLE Express (Life Technologies, Thermo Fisher) for 5 minutes at 37°C before being neutralized in RPMI 1640 medium containing 10% FBS, and passed through 18G needles to 70 μm cell strainers. Samples were incubated in ACK (ammonium-chloride-potassium) lysis buffer for 5 minutes at RT before flooding with phosphate buffered saline (PBS) and spinning down. Single-cell suspension was incubated in Zombie Viability Dye (BioLegend) for 10 to 15 minutes and spun down. Antibody cocktail (CD45-FITC, EpCAM-PE, CD26-APC, and CD49f-BV421, 1:100 dilution; BioLegend) was added to cells followed by incubation at 4°C for 30 minutes in the dark. Cells were filtered and sorted on BD FACSARIA (BD Biosciences, San Jose, CA) for luminal (CD45−, EpCAM+, CD26+, and CD49f−) and basal (CD45−, EpCAM+, CD26−, and CD49f+) cells. Sorted cells were washed with PBS and immediately suspended in TRIzol Reagent (Thermo Fisher) for subsequent RNA and protein isolation according to manufacturer's protocols.

2.6 | Immunoblot

Proteins were separated on NuPAGE 4% to 12% Bis-Tris gels (Thermo Fisher) and transferred to nitrocellulose membrane (Bio-Rad Laboratories, Hercules, CA). The membrane was blocked in TBST (Tris-buffered saline with 0.2% Tween-20) with 5% milk for 1 hour and incubated with primary antibodies diluted (1:1000) in TBST with 2% milk overnight at 4°C and secondary antibodies (Thermo Fisher) (diluted 1:10 000) for 1 hour at RT. The following primary antibodies were used: mouse anti-SULT2B1 (Abcam, #ab88085), rabbit anti-CK5 (BioLegend) and mouse anti-glyceraldehyde-3-phosphate dehydrogenase (GAPDH) (Invitrogen). The membrane was developed using SuperSignal West Pico PLUS Chemiluminescent Substrate (Thermo Fisher). Images were taken using ChemiDoc Touch Imaging System (Bio-Rad) and desitometry analysis was performed using Image Lab software (Bio-Rad).

2.7 | Real Time-PCR (RT-PCR)

Total RNA was isolated using TRIzol Reagent (Thermo Fisher) according to the manufacturer's protocol. cDNA was synthesized with M-MuLV Reverse Transcriptase (New England Biolabs, Ipswich, MA) as described previously.[18] Quantitative real-time polymerase chain reaction (qRT-PCR) was conducted on LightCycler 96 (Roche, Basel, Switzerland) using PerfeCTa qPCR FastMix II (Quantabio, Beverly, MA) according to the manufacturer's protocol. PrimeTime qPCR Assay probes specific for human *SULT2B1b* (Hs.PT.58.22508626) or for mouse *Sult2b1* (Mm.PT.58.5982373) (Integrated DNA Technologies, Skokie, IL) were used and the transcript levels were normalized using TaqMan Ribosomal RNA Control Reagents (Thermo Fisher).

2.8 | Prostate organoid culture

The animal protocols used in this study were approved by Purdue Animal Care and Use Committee. The prostate stem cell population was isolated as previously described.[21,22] Briefly, minced prostate tissue from 8 to 12 week-old mice was digested with 1mg/mL Collagenase-I (Sigma-Aldrich) in RPMI 1640 medium with 10% FBS for 2 hours, followed by trypsinization at 37°C. Isolated cells were stained with Zombie Viability Dye (BioLegend) for 10 to 20 minutes at RT and then incubated with an antibody cocktail

including Sca1-APC, CD49f-PE, CD45-FITC, and CD31-FITC (BioLegend) for 30 minutes at 4°C. Lineage-negative (CD45−CD31−), Sca1+, and CD49f+ (LSC) live cell sorting was performed on the BD FACSARIA (BD Biosciences) in sterile condition. Sorted population was gently resuspended in 1:2 prostate epithelial growth medium (PrEGM) (Lonza, Basel, Switzerland)/Matrigel (Corning) and seeded at a density of 10 000 cells/well in 12-well plates and incubated for 7 days with two media changes. Organoids formed from primary culture were released by incubating with 1 mg/mL Dispase (Invitrogen) at 37°C for 1 hour. Cells were washed in PBS and immediately suspended in TRIzol Reagent (Thermo Fisher) for subsequent RNA and protein isolation according to manufacturer's protocol.

2.9 | Statistical analyses

The values from two groups were compared using Student t test, and values from multiple groups were compared using one-way analysis of variance (ANOVA; Prism, GraphPad, San Diego, CA). SULT2B1b staining intensities were compared using the nonparametric Mann-Whitney *U* test (Prism, GraphPad). Values of $P < 0.05$ were considered statistically significant. Data are presented as means ± SEM.

3 | RESULTS

3.1 | SULT2B1b is localized in the prostate epithelium

A stable cell line derived from LNCaP human prostate cancer cells that expresses doxycycline-inducible SULT2B1b[18] was used as a positive control for the antibody used for immunohistochemistry (IHC). As shown in Figure 1A, SULT2B1b staining intensity was markedly elevated in inducible cells treated with doxycycline, consistent with SULT2B1b induction previously shown by immunoblot.[18] SULT2B1b IHC was then conducted on human prostate tissue samples. It was only detected in the prostate epithelium, absent in any of the stromal components, such as the fibroblasts and endothelial cells (Figure 1B, left panel). It was not detected in leukocytes either, as shown with human BPH tissues with inflammation (Figure 1B, right panel). The specific expression of SULT2B1b in the epithelium was consistent in both normal prostate and BPH samples. Subcellularly, SULT2B1b was detected in the cytoplasm, consistent with what has been previously reported.[23]

3.2 | SULT2B1b decreases in advanced prostate Cancer

We next examined SULT2B1b with IHC in prostate cancer tissue microarrays which contain paired primary tumor tissues and normal prostate tissues from the same patients. SULT2B1b staining intensity was found to be much weaker in cancer cells than in adjacent normal epithelial cells (Figure 2A). SULT2B1b IHC was also conducted on a tissue microarray which consists of prostate metastases at distant organs including bone, liver, lung, and lymph nodes. Interestingly, little to no SULT2B1b was detected in these prostate metastases, regardless of the organ sites (Figure 2B). Grading of the IHC staining intensity confirmed the significant reduction of SULT2B1b in primary prostate tumors and a further reduction in metastases as compared with normal prostate epithelium (Figure 2C), demonstrating that SULT2B1b inversely correlates with prostate cancer progression, with the highest level in normal epithelium and lowest in advanced metastatic prostate cancer. Furthermore,

SULT2B1b was also found to associate with other markers for malignant prostate cancer. For example, although the differences did not reach any statistical significance, SULT2B1b staining intensity was lower in recurrent prostate tumor samples than nonrecurrent samples (recurrent, 0.88 ± 0.23; nonrecurrent, 1.32 ± 0.25; $P = 0.15$) and lower in tumor samples with higher Gleason score (Gleason score of more than 3, 0.50 ± 0.21; Gleason score of 3, 1.13 ± 0.22; $P = 0.18$).

This inverse relationship between SULT2B1b and prostate cancer was also confirmed at the transcript level. Analysis of RNA-seq data downloaded from TCGA has revealed that SULT2B1 mRNA was significantly lower in prostate tumor samples than in normal samples (Figure 2D). Survival analysis of the TCGA data also found a trend towards shorter patient survival in samples with lower SULT2B1 expression ($P = 0.141$), which is consistent with the data from the Human Protein Atlas (www.proteinatlas.org). Data in the Protein Atlas showed a significant correlation between low SULT2B1 expression and shorter 5-year survival ($P = 0.044$). Overall, these data indicate that prostate cancer cells lose SULT2B1b expression as they become more malignant and metastatic.

3.3 | SULT2B1b staining is more concentrated in the luminal layer of prostate epithelium

Not only did we find that SULT2B1b was only expressed in the epithelium of normal prostate and BPH samples, we also noticed that SULT2B1b was mainly localized in the luminal layer of the epithelium. As shown in Figure 3A, strong SULT2B1b IHC staining was present in the luminal epithelial cells whereas the staining was much weaker or even absent in the basal layer (arrows). The difference between the two epithelial layers can be observed in normal prostate as well as BPH samples with glandular or basal hyperplasia (Figure 3A). Quantitation of the staining intensity confirmed the significant difference in SULT2B1b between the luminal and basal layer with the luminal layer expressing about 3 to 4 fold higher SULT2B1b than the basal layer (Figure 3B). Consistent with our findings, an analysis of bulk sequencing from CD26 + luminal epithelia and CD271 + basal epithelia showed a significant enrichment of SULT2B1 in luminal epithelia.[10]

Next, we confirmed the luminal localization of SULT2B1b by costaining with the luminal marker Cytokeratin 8 (CK8) and the basal marker Cytokeratin 5 (CK5). The staining pattern of SULT2B1b matched that of CK8 while showing little overlap with CK5 in normal prostate tissues (Figure 4A) and BPH tissues with glandular hyperplasia (Figure 4B), demonstrating that SULT2B1b is indeed most highly expressed in the luminal epithelial cells. Interestingly, in BPH samples with basal hyperplasia, weak CK8 staining was found in CK5 + basal cells (Figure 4C, arrowheads). Again, weak SULT2B1b staining could be detected in the same basal cells with weak CK8 staining (Figure 4C). The presence of these CK8+, SULT2B1b+, and CK5+ cells suggests that the basal cells in basal hyperplasia may acquire some of the luminal characteristics.

3.4 | SULT2B1b expression is significantly higher in prostate luminal epithelial cells and is induced in prostate organoids

We sorted basal and luminal cells with specific markers (CD49f and CD26, respectively) from 11 human BPH samples and analyzed SULT2B1b expression in these paired samples.

As shown in the immunoblots with all the samples (Figure 5A), SULT2B1b protein was increased in the luminal population. CK5 immunoblot confirmed the identity of the sorted basal population. Considering the difference in the quantity of total protein loaded for these immunoblots, SULT2B1b levels as quantified with densitometry were further normalized to those of the loading control GAPDH. SULT2B1b protein was found to be significantly higher in the sorted luminal population than in the basal population (Figure 5B). RT-PCR was also performed with the same set of samples to evaluate SULT2B1b at the transcript level (Figure 5C). Although there was some variability in its expression in the basal and luminal populations from different patients, increased SULT2B1b was found in the majority of luminal populations compared with basal populations.

The distinct expression pattern of SULT2B1b in the prostate epithelium suggests that this protein may be implicated in the differentiation of the luminal layer. To test this possibility, lineage-negative (CD45−CD31−), Sca1+, and CD49f+ (LSC) cells which have been identified as prostate stem cells[24] were isolated from mouse prostates and allowed to form organoids in Matrigel matrix as previously reported.[22] We have previously shown that the prostate organoids cultured from LSC cells exhibited multilineage differentiation and started expressing the luminal marker CK8 which was absent in the precursor LSC cells.[22] Given that the primers specific for mouse SULT2B1b isoform were not available, total SULT2B1 expression was analyzed instead and compared between the precursor LSCs and organoids. It was found that SULT2B1 transcript was significantly upregulated in the prostate organoids (Figure 5D). Among the samples analyzed, there were two matched pairs of LSC cells and the organoids grown from the same population. SULT2B1 was remarkably induced in prostate organoids as compared with their matched precursors (Figure 5E).

4 | DISCUSSION

We have reported here an inverse correlation between SULT2B1b expression and prostate cancer status, with the highest SULT2B1b levels in normal prostate and BPH, intermediate levels in primary prostate tumors and the lowest levels in advanced metastatic prostate cancer. Reduced SULT2B1b in primary prostate tumors has also been reported by Seo et al.[25] We confirmed their findings with a larger cohort of primary prostate tumor samples and compared SULT2B1b staining intensity in the tumor tissues with paired normal prostate tissues from the same patient. Importantly, we have also included metastatic prostate samples in our study and found that the levels of SULT2B1b in these distant metastases were further reduced compared with those in primary tumors, which has not been described previously. In addition, by analyzing the data from TCGA, we have demonstrated with 497 prostate tumor samples that the difference in SULT2B1b between normal prostate and prostate tumors also exists at the transcript level. Furthermore, by incorporating the clinical data of patient specimens analyzed, we observed a trend of reduced SULT2B1b in recurrent prostate cancer compared with nonrecurrent cancer and a trend of reduced SULT2B1b in tumor samples with higher Gleason scores. The TCGA data have also shown a trend between lower SULT2B1b expression and shorter patient survival. Combined together, all these data indicated that lower SULT2B1b is associated with markers or characteristics of malignant prostate cancer (eg, distant metastasis, recurrence, higher Gleason score, and poor outcome). Interestingly, despite the low level of SULT2B1b in prostate cancer, it does appear

to be essential for the survival of cancer cells, as our group has previously demonstrated that SULT2B1b downregulation induces cell death in prostate cancer cells.[18]

The most important finding from our study, one that has not been described before, is that the luminal layer of the prostate epithelium exhibits a much higher SULT2B1b level than the basal layer. It has been confirmed, both at the transcript and protein level, with both human prostate tissue samples and sorted luminal and basal cell populations. This observation has been consistent across normal prostate and BPH with different phenotypes (ie, glandular and basal hyperplasia). The next logical question to ask would be why SULT2B1b is overexpressed in the prostate luminal epithelium. One possible answer could be that it is critical for the differentiation of the luminal layer. In support of this hypothesis, our data with prostate cancer have shown that SULT2B1b correlates with the differentiation status of the prostate epithelium. For example, fully differentiated prostate epithelium in normal prostate and BPH showed the strongest SULT2B1b expression, whereas it was barely expressed in prostate cancer metastases in which most cancer cells exhibited an undifferentiated phenotype (Figure 2B). SULT2B1b in primary prostate tumors with recognizable glandular structures was expressed at a level between normal prostate and prostate cancer metastasis (Figure 2A and 2C). Another piece of evidence in this study that supports the hypothesis is that SULT2B1 was induced in more differentiated prostate organoids with luminal properties as compared to the stem cell population LSC (Figure 5D and 5E). The association between SULT2B1b (or its product CS) and differentiation has also been reported in skin epidermis[6] and airway epithelial cells.[26] Another potential function of SULT2B1b in the prostate epithelium is that it may be critical for the homeostasis and maintenance of the epithelial cells, as we have found that the viability of RWPE-1, a normal prostate epithelial cell line, decreased with reduced SULT2B1b expression.[18]

AR has been shown to be essential for the differentiation and homeostasis of prostate luminal epithelium.[27,28] We have previously shown in prostate cancer cells that SULT2B1b knockdown inhibits AR expression and signaling.[18] Therefore one of the potential mechanisms may be that SULT2B1b contributes to luminal cell differentiation or maintenance by modulating the AR pathway.

Although SULT2B1b is exclusively expressed in the prostate epithelium, it may potentially influence the microenvironment through its products such as CS. CS, which is produced in the Harderian gland in the eye, binds directly to DOCK2 and inhibits leukocyte migration and activation by blocking DOCK2 activity, therefore contributing to the immunosuppressive environment in the eye.[9] CS may also inhibit T cell function by displacing cholesterol from cell membrane and therefore compromising T cell receptor signaling.[8] SULT2B1b may also alter the surrounding vasculature by modulating the production of angiogenic factors such as VEGF.[29] Thus, the high level of SULT2B1b in the prostate epithelium may not only be beneficial for the epithelium but also be important for the stability of the tissue microenvironment.

5 | CONCLUSIONS

In summary, our study has examined the expression pattern of SULT2B1b in the prostate across a spectrum of pathological conditions, including BPH with glandular and basal hyperplasia, primary prostate tumor, and distant metastases. We have found a strong negative correlation between SULT2B1b and prostate cancer, and a strong positive correlation between SULT2B1b and epithelial differentiation.

Supplementary Material

Refer to Web version on PubMed Central for supplementary material.

ACKNOWLEDGEMENTS

These studies were supported by the Department of Defense Prostate Cancer Program (W81XWH-14-1-058830), the Purdue University Center for Cancer Research (NIH grant P30 CA023168), and the Walther Cancer Foundation. The authors acknowledge the assistance of Flow Cytometry and Cell Separation Facility of the Bindley Bioscience Center and Purdue University Histology Research Laboratory, both of which are core facilities of the NIH-funded Indiana Clinical and Translational Science Institute. The authors also thank the patients and their families, Drs. Celestia Higano, Evan Yu, Pete Nelson, Bruce Montgomery, Elahe Mostaghel, Paul Lange, Bill Ellis, Dan Lin, Xiaotun Zhang, Martine Roudier, Lawrence True, Robert Vessella, and the rapid autopsy teams for their contributions to the University of Washington Medical Center Prostate Cancer Donor Rapid Autopsy Program. The material from the University of Washington was the result of work supported by resources by the Pacific Northwest Prostate Cancer SPORE (P50CA97186), the PO1 NIH grant (PO1CA163227), and the Institute for Prostate Cancer Research.

Funding information

National Institutes of Health, Grant/Award Number: P30 CA023168 (TLR); U.S. Department of Defense, Grant/Award Number: W81XWH-14-1-058830 (TLR); Walther Cancer Foundation (TLR); Pacific Northwest Prostate Cancer SPORE, Grant/Award Number: P50CA97186 (CM); National Institutes of Health, Grant/Award Number: P01CA163227 (CM)

REFERENCES

1. Her C, Wood TC, Eichler EE, et al. Human hydroxysteroid sulfotransferase SULT2B1: two enzymes encoded by a single chromosome 19 gene. Genomics. 1998;53(3):284–295. [PubMed: 9799594]
2. Falany CN, Rohn-Glowacki KJ. SULT2B1: unique properties and characteristics of a hydroxysteroid sulfotransferase family. Drug Metab Rev. 2013;45(4):388–400. [PubMed: 24020383]
3. Javitt NB, Lee YC, Shimizu C, Fuda H, Strott CA. Cholesterol and hydroxycholesterol sulfotransferases: identification, distinction from dehydroepiandrosterone sulfotransferase, and differential tissue expression. Endocrinology. 2001;142(7):2978–2984. [PubMed: 11416019]
4. Fuda H, Javitt NB, Mitamura K, Ikegawa S, Strott CA. Oxysterols are substrates for cholesterol sulfotransferase. J Lipid Res. 2007;48(6):1343–1352. [PubMed: 17347498]
5. Chen W, Chen G, Head DL, Mangelsdorf DJ, Russell DW. Enzymatic reduction of oxysterols impairs LXR signaling in cultured cells and the livers of mice. Cell Metab. 2007;5(1):73–79. [PubMed: 17189208]
6. Elias PM, Williams ML, Choi EH, Feingold KR. Role of cholesterol sulfate in epidermal structure and function: lessons from X-linked ichthyosis. Biochim Biophys Acta. 2014;1841(3):353–361. [PubMed: 24291327]
7. Heinz L, Kim GJ, Marrakchi S, et al. Mutations in SULT2B1 cause autosomal-recessive congenital ichthyosis in humans. Am J Hum Genet. 2017;100(6):926–939. [PubMed: 28575648]
8. Wang F, Beck-Garcia K, Zorzin C, Schamel WW, Davis MM. Inhibition of T cell receptor signaling by cholesterol sulfate, a naturally occurring derivative of membrane cholesterol. Nat Immunol. 2016;17(7):844–850. [PubMed: 27213689]

9. Sakurai T, Uruno T, Sugiura Y, et al. Cholesterol sulfate is a DOCK2 inhibitor that mediates tissue-specific immune evasion in the eye. Sci Signal. 2018;11(541):eaao4874. [PubMed: 30065028]
10. Henry GH, Malewska A, Joseph DB, et al. A cellular anatomy of the normal adult human prostate and prostatic urethra. Cell Rep. 2018;25(12):3530–3542. [PubMed: 30566875]
11. Verhagen AP, Ramaekers FC, Aalders TW, Schaafsma HE, Debruyne FM, Schalken JA Colocalization of basal and luminal cell-type cytokeratins in human prostate cancer. Cancer Res. 1992;52(22):6182–6187. [PubMed: 1384957]
12. Strand DW, Costa DN, Francis F, Ricke WA, Roehrborn CG. Targeting phenotypic heterogeneity in benign prostatic hyperplasia. Differentiation. 2017;96:49–61. [PubMed: 28800482]
13. Henry G, Malewska A, Mauck R, et al. Molecular pathogenesis of human prostate basal cell hyperplasia. Prostate. 2017;77(13):1344–1355. [PubMed: 28795417]
14. Thorson P, Swanson PE, Vollmer RT, Humphrey PA. Basal cell hyperplasia in the peripheral zone of the prostate. Mod Pathol. 2003;16(6):598–606. [PubMed: 12808066]
15. Attard G, Parker C, Eeles RA, et al. Prostate cancer. Lancet. 2016;387(10013):70–82. [PubMed: 26074382]
16. Zhang D, Park D, Zhong Y, et al. Stem cell and neurogenic gene-expression profiles link prostate basal cells to aggressive prostate cancer. Nat Commun. 2016;7:10798. [PubMed: 26924072]
17. Zhao SG, Chang SL, Erho N, et al. Associations of luminal and basal subtyping of prostate cancer with prognosis and response to androgen deprivation therapy. JAMA Oncol. 2017;3(12):1663–1672. [PubMed: 28494073]
18. Vickman RE, Crist SA, Kerian K, et al. Cholesterol sulfonation enzyme, SULT2B1b, modulates AR and cell growth properties in prostate cancer. Mol Cancer Res. 2016;14(9):776–786. [PubMed: 27341831]
19. Anders S, Pyl PT, Huber W. HTSeq--a Python framework to work with high-throughput sequencing data. Bioinformatics. 2015;31(2):166–169. [PubMed: 25260700]
20. Strand DW, Aaron L, Henry G, Franco OE, Hayward SW. Isolation and analysis of discreet human prostate cellular populations. Differentiation. 2016;91(4-5):139–151. [PubMed: 26546040]
21. Lukacs RU, Goldstein AS, Lawson DA, Cheng D, Witte ON. Isolation, cultivation and characterization of adult murine prostate stem cells. Nat Protoc. 2010;5(4):702–713. [PubMed: 20360765]
22. Wang HH, Wang L, Jerde TJ, et al. Characterization of autoimmune inflammation induced prostate stem cell expansion. Prostate. 2015;75(14):1620–1631. [PubMed: 26174474]
23. He D, Meloche CA, Dumas NA, Frost AR, Falany CN. Different subcellular localization of sulphotransferase 2B1b in human placenta and prostate. Biochem J. 2004;379(Pt 3):533–540. [PubMed: 14741047]
24. Lawson DA, Xin L, Lukacs RU, Cheng D, Witte ON. Isolation and functional characterization of murine prostate stem cells. Proc Natl Acad Sci U S A. 2007;104(1):181–186. [PubMed: 17185413]
25. Seo YK, Mirkheshti N, Song CS, et al. SULT2B1b sulfotransferase: induction by vitamin D receptor and reduced expression in prostate cancer. Mol Endocrinol. 2013;27(6):925–939. [PubMed: 23579488]
26. Rearick JI, Hesterberg TW, Jetten AM. Human bronchial epithelial cells synthesize cholesterol sulfate during squamous differentiation in vitro. J Cell Physiol. 1987;133(3):573–578. [PubMed: 3480290]
27. Xie Q, Liu Y, Cai T, Horton C, Stefanson J, Wang ZA. Dissecting cell-type-specific roles of androgen receptor in prostate homeostasis and regeneration through lineage tracing. Nat Commun. 2017;8:14284. [PubMed: 28112153]
28. Wu CT, Altuwaijri S, Ricke WA, et al. Increased prostate cell proliferation and loss of cell differentiation in mice lacking prostate epithelial androgen receptor. Proc Natl Acad Sci U S A. 2007;104(31):12679–12684. [PubMed: 17652515]
29. Chen W, Zhou H, Ye L, Zhan B. Overexpression of SULT2B1b promotes angiogenesis in human gastric cancer. Cell Physiol Biochem. 2016;38(3):1040–1054. [PubMed: 26937945]

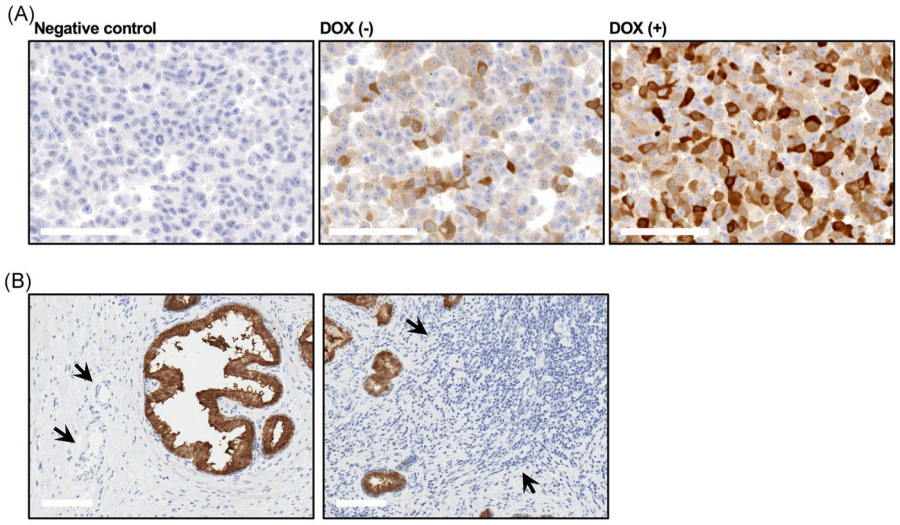

FIGURE 1.

SULT2B1b is localized in the prostate epithelium. A, LNCaP human prostate cancer cells with doxycycline-inducible SULT2B1b were used as the positive control for immunohistochemistry (IHC). Negative control: primary antibody replaced with mouse IgG. Dox (+): cells treated with doxycycline. Scale bar, 100 μm. B, In human benign prostate hyperplasia (BPH) samples, SULT2B1b was only found in the epithelium, not in the stroma. Staining was negative in fibroblasts, endothelial cells (left panel; arrows point to blood vessels) and leukocytes (right panel; arrows point to an area enriched with leukocytes). Scale bar, 100 μm. SULT2B1b, sulfotransferase family 2B member 1b. [Color figure can be viewed at wileyonlinelibrary.com]

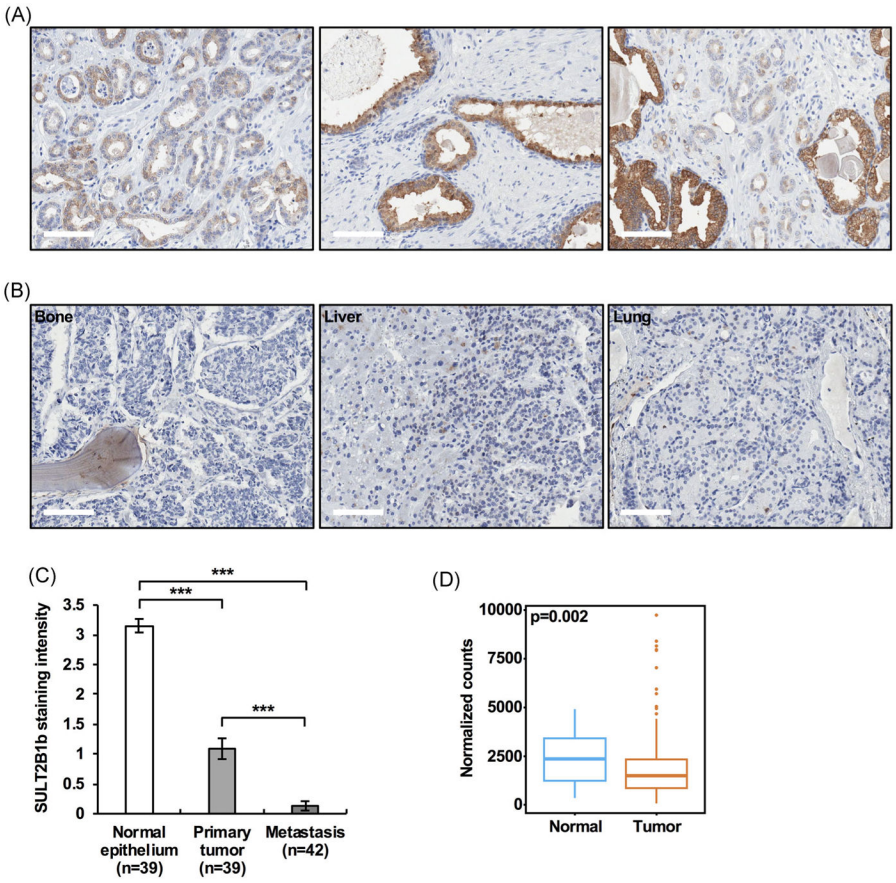

FIGURE 2.

SULT2B1b level decreases in prostate cancer. A, Representative microscopic images are shown for SULT2B1b immunohistochemistry in prostate cancer cells (left panel) and adjacent normal prostate epithelium (middle panel). Prostate cancer cells are also shown together with neighboring normal epithelium (right panel). Scale bar, 100 μm. B, Representative microscopic images are shown for SULT2B1b staining in prostate cancer metastases in distant organs, such as bone, liver, and lung. Scale bar, 100 μm. C, Quantitation of SULT2B1b staining intensity in normal prostate epithelium, primary and metastatic prostate cancer cells. Total number of samples analyzed in each group is indicated. In the metastasis group, two samples were analyzed for each of the 21 patients, with one from bone metastasis and the other from other organ metastasis. ***$P < 0.001$. D, SULT2B1 transcript is also expressed at a significantly lower level in prostate tumor samples than normal prostate samples, as shown by analysis of TCGA data from 52 normal and 497 tumor samples. SULT2B1b, sulfotransferase family 2B member 1b. [Color figure can be viewed at wileyonlinelibrary.com]

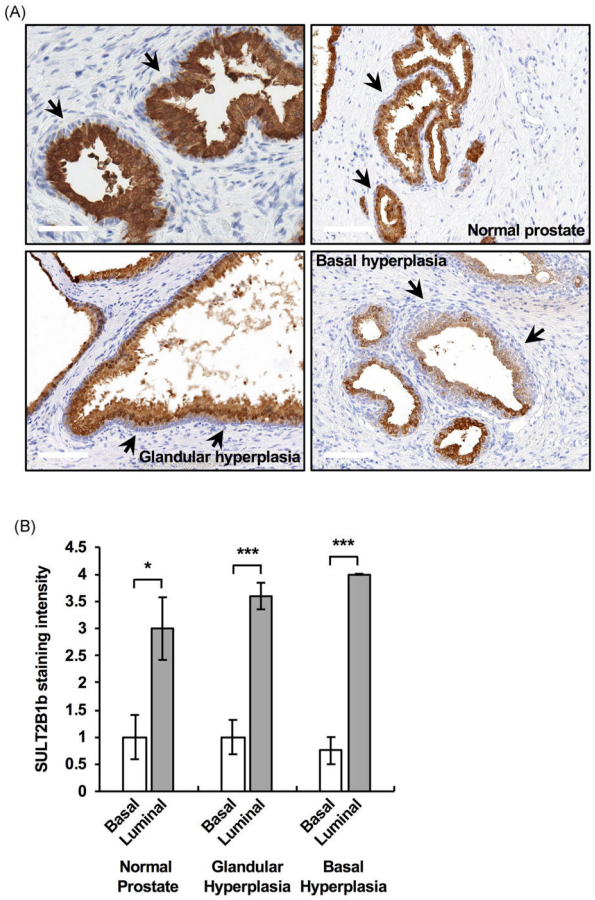

FIGURE 3.

SULT2B1b staining is more concentrated in luminal prostate epithelial cells. A, Stronger SULT2B1b staining was detected in luminal epithelial cells (upper left; scale bar, 50 μm). This expression pattern was observed in normal prostate (upper right; scale bar, 100μm) and benign prostate hyperplasia (BPH) with different phenotypes, for example, glandular hyperplasia (lower left; scale bar, 100μm) and basal hyperplasia (lower right; scale bar, 100 μm). Arrows point to the basal layer with weaker SULT2B1b staining. B, Quantitation of SULT2B1b staining intensity in basal and luminal epithelial cells of normal prostate (n = 4) and BPH samples (glandular hyperplasia, n = 5; basal hyperplasia, n = 4). SULT2B1b, sulfotransferase family 2B member 1b. *P< 0.05, ***P < 0.001. [Color figure can be viewed at wileyonlinelibrary.com]

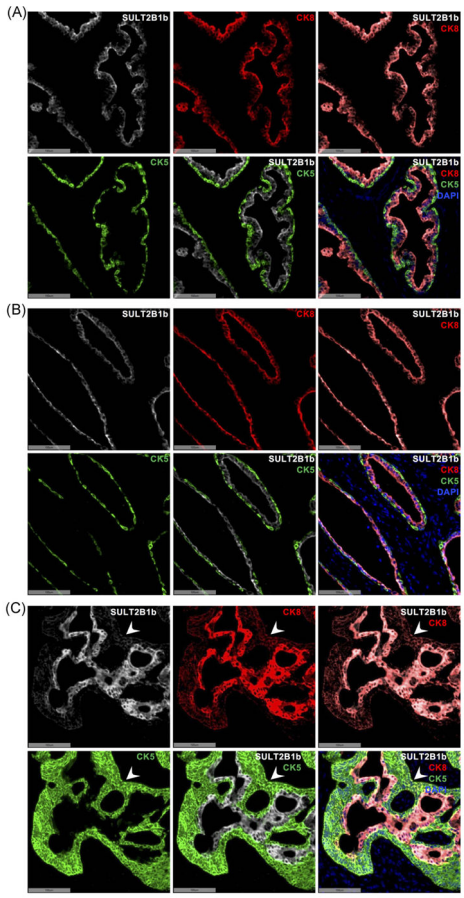

FIGURE 4.

SULT2B1b colocalizes with the luminal epithelial marker. Representative microscopic images are shown for normal human prostate tissues (A), benign prostate hyperplasia tissues with glandular hyperplasia (B) or with basal hyperplasia (C), costained with CK8 (luminal marker, red), CK5 (basal marker, green), SULT2B1b (white), and DAPI (nuclear staining, blue). As shown in the composite images with CK8/SULT2B1b, or with CK5/SULT2B1b staining, SULT2B1b is mostly colocalized with CK8, not with CK5. Arrowheads point to an area in the basal layer that showed weak staining of both SULT2B1b and CK8. Scale bar, 100 μm. DAPI, 4',6-diamidino-2-phenylindole; SULT2B1b, sulfotransferase family 2B member 1b. [Color figure can be viewed at wileyonlinelibrary.com]

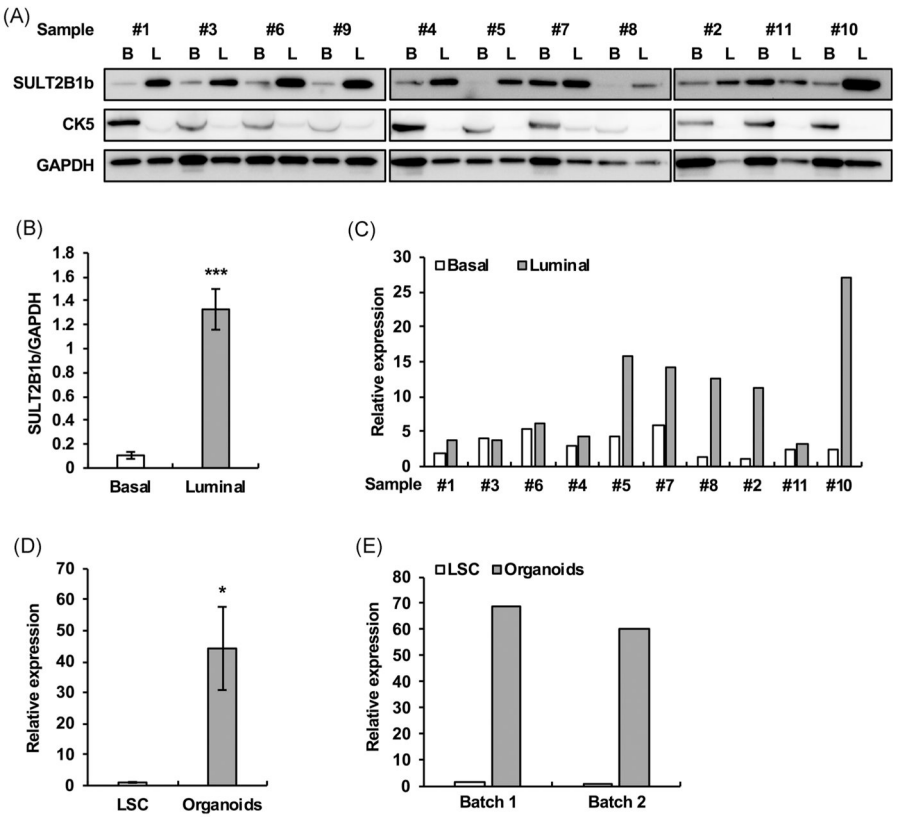

FIGURE 5.

SULT2B1b expression is significantly higher in sorted luminal prostate epithelial cells than basal epithelial cells and is induced with prostate organoid formation. Prostate epithelial cells from 11 human benign prostate hyperplasia samples were sorted into basal (B) and luminal (L) populations. SULT2B1b expression in these paired samples was analyzed with both immunoblot (A) and RT-PCR (C). CK5 was used in the immunoblot to confirm the identity of the sorted basal cell population. RT-PCR was not performed on sample #9 due to insufficient RNA. Intensity of protein bands in (A) was quantified with densitometry (n = 11) (B). Intensity of SULT2B1b bands was normalized to that of GAPDH (glyceraldehyde-3-phosphate dehydrogenase) bands. ***P <0.001. D, SULT2B1 expression was increased in mouse prostate organoids compared to the prostate stem cell population (LSC) as analyzed by RT-PCR (LSC, n = 14; organoids, n = 5). *P < 0.05. E, Increased SULT2B1 expression in prostate organoids is shown in two independent batches of mouse prostate organoids and their matched precursor LSC cells. RT-PCR, real-time polymerase chain reaction; SULT2B1b, sulfotransferase family 2B member 1b.